Available online at www.sciencedirect.com

ScienceDirect

Procedia Materials Science 3 (2014) 924 – 929

Procedia Materials Science

www.elsevier.com/locate/procedia

20th European Conference on Fracture (ECF20)

Fatigue limit prediction of large scale cast aluminum alloy A356

Akiko Tajiri[a], Taishi Nozaki[b], Yoshihiko Uematsu[b], Toshifumi Kakiuchi[b], Masaki Nakajima[c], Yuki Nakamura[c], Hiroshi Tanaka[a]

[c]*Murata Machinery Ltd., 2 Nakajima, Hashizume, Inuyama, Aichi 484-8502, Japan*

[b]*Gifu University, 1-1 Yanagido, Gifu 501-1193, Japan*

[c]*Toyota National College of Technology, 2-1 Eisei-cho, Toyota, Aichi 471-8525, Japan*

Abstract

Casting defects such as gas pores and shrinkages typically occur during casting process. These casting defects affect fatigue crack initiation and strongly dominate fatigue strength. Particularly, in a large scale component, the molten metal flow is complicated and the cooling rate is dependent on the locations, which affect the formation of casting defects. In the present study, rotating bending fatigue tests of cast aluminum alloy A356 were conducted using the specimens sampled at three locations of a large scale component where the cooling rates were different. The fatigue limit was predicted based on the statistics of casting defect size and compared with the experimental results. Fractographic analyses revealed fatigue crack initiated from casting defect in all specimens. Murakami et al. suggested the method for predicting the fatigue limit of steel using the extreme value statistics of inclusion size (Murakami et al., 1989). Ueno et al. modified Murakami's equation and proposed the equations to predict the fatigue limit of die-cast aluminum alloy based on the defect size (Ueno et al., 2012). The present authors suggest the modified evaluation method of defect size considering the combination of the neighboring defects which exist near to each other. The predictions agree well with the experimental results but they are slightly different, which indicates the other metallurgical factors affect fatigue strength.

Selection and peer-review under responsibility of the Norwegian University of Science and Technology (NTNU), Department of Structural Engineering

Keywords: Fatigue; Cast aluminum alloy; Fatigue life prediction; Casting defect; Extreme value statistics

1. Introduction

Recently, high reliable design at low cost has been required in the background of such as energy problems. So the

* Corresponding author. Tel.: +81-58-293-2501; fax: +81-58-293-2491.
E-mail address: yuematsu@gifu-u.ac.jp

Selection and peer-review under responsibility of the Norwegian University of Science and Technology (NTNU), Department of Structural Engineering
doi:10.1016/j.mspro.2014.06.150

cast aluminum alloy, which has a high specific strength and is relatively inexpensive, is used widely for the structural material. The cast alloy inevitably has casting defects such as gas holes and shrinkages in itself. These casting defects affect fatigue properties. As the previous studies on the relationship between fatigue limit and inclusion size in steel, Murakami's √area parameter model (Murakami et al., 1989) is well known. In Murakami's model, the maximum size of defect, √area, is estimated by the extreme value statistics and the fatigue limit is calculated using the equations which have the terms of √area and Vickers hardness. Ueno et al. applied this model to die-cast aluminum alloy with the artificial defects and they proposed the modified equations empirically appropriate for the aluminum alloy (Ueno et al., 2012). However, the defect distributions in a large scale ingot of cast aluminum alloy and the correlation of defects have not been studied in detail.

In this study, the fatigue tests were conducted using specimens which were sampled from the different locations of the large scale cast aluminum alloy A356. The validity of the fatigue limit prediction method based on Ueno's modified √area parameter model and the effect of casting defects distribution resulting from the complicated molten metal flow and cooling during casting process on the fatigue behavior was investigated.

2. Material and experimental procedure

2.1. Material and specimen

Material used in this study was cast aluminum alloy A356. The chemical composition of material is shown in Table 1. The large scale ingot with the size of 1.5 m in length, 0.6 m in height and 0.5 m in width was prepared by casting process. In a large component, the molten metal flow is complicated and the cooling rates are dependent on the location. The molten metal flow and the cooling rates were predicted by the casting simulation and the materials were sampled from three locations where the cooling rates were different. The materials are denoted as material A, B and C in the order of the cooling rates. The cooling rate of material A is the fastest and that of material C is the lowest. The pouring gates, from which the molten metal was poured, were placed at multiple sites in the upper side of casting die. Material A was sampled from the bottom area of the ingot far from the pouring gates. Material B and C were sampled at the lower and the upper areas of the ingot just below one of the pouring gates. The fatigue specimens having a gauge section of 10 mm length and 8 mm diameter were machined from each material to the configuration shown in Fig.1. Before the fatigue tests, the specimens were mechanically polished using emery papers and finished to mirror surface by buffing.

Table 1 Chemical composition of material (wt%)

Si	Mg	Fe	Ni	Cr	Sn	Al
6.66	0.383	0.153	0.009	0.002	0.002	Bal.

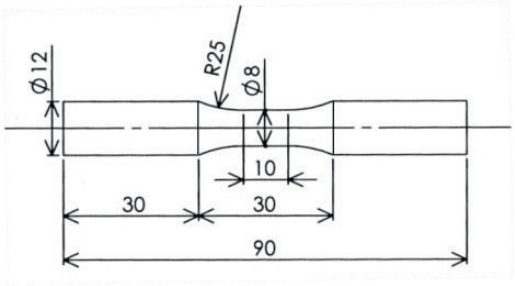

Fig.1 Fatigue specimen configuration.

2.2. Experimental procedures

The microstructures were observed by optical microscope. Before the microstructure observation, the material was etched with the etching liquid which was composed of 5 ml hydrochloric acid, 7.5 ml hydrofluoric acid and 4.5 ml distilled water. The hardness test was conducted by micro Vickers hardness tester under a load of 0.98 N and a holding time of 30 s. Tensile test was conducted by universal material testing machine. Fatigue tests were conducted by four-point rotating bending fatigue testing machine under a load ratio of $R = \sigma_{min}/\sigma_{max} = -1$ and a frequency of 60 Hz at room temperature. Fatigue limit σ_w was defined as the upper limit stress at which the specimen survived after the number of cycles N=10^7. All of the fracture surfaces were examined in detail by a scanning electron microscope (SEM).

3. Results

3.1. Mechanical properties and microstructure observation

Mechanical properties of material A is shown in Table 2. Vickers hardness of material A, B and C were 116, 108 and 90 HV, respectively. Fig.2 shows the microstructures of the materials. The dendrite structure was widely distributed. The dendrite arm spacing (DAS) increased in the order of material A, B and C with decreasing cooling rate. The DAS were 57, 84 and 96 μm, respectively. As seen in Fig.2, the casting defects were observed in the microstructures. The sizes of casting defects were various and scattered in a wide range.

Table 2 Mechanical properties of material A.

0.2% proof stress $\sigma_{0.2}$ (MPa)	Tensile stress σ_B (MPa)	Elongation δ(%)	Elastic modulus E (GPa)
215	237	2.5	70

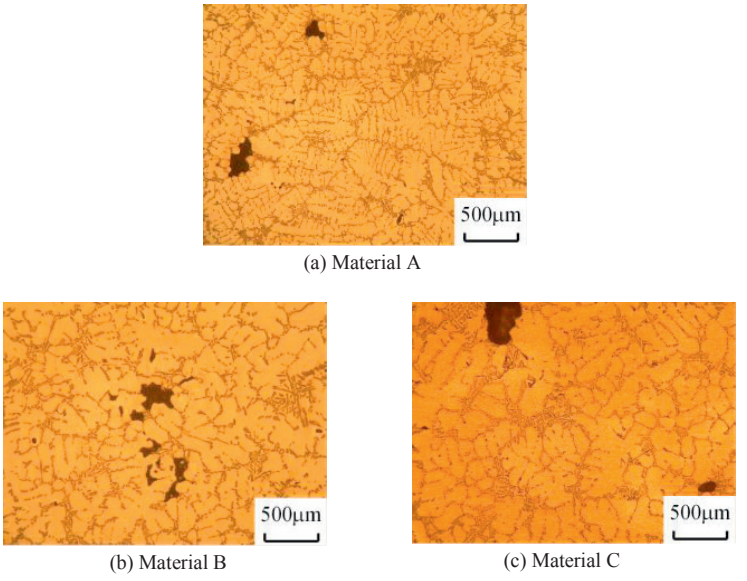

(a) Material A

(b) Material B

(c) Material C

Fig.2 Microstructure of materials.

3.2. Fatigue strength

The *S-N* diagram is shown in Fig.3. The fatigue strengths of all the materials in the finite life region are nearly the same. On the other hand, the fatigue limits are different among the three materials. The fatigue limits of material A, B and C were 65, 80 and 75 MPa, respectively.

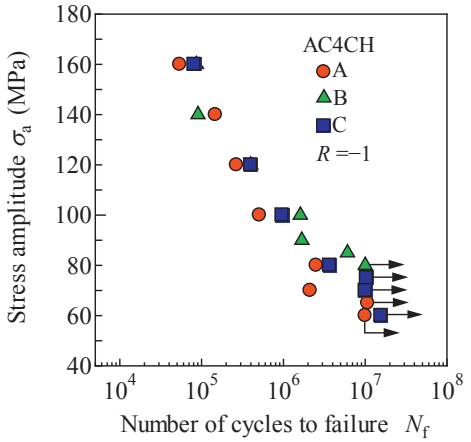

Fig.3 *S-N* diagram.

3.3. Fracture surface

SEM micrographs showing the fracture surface of material A near the crack initiation site are shown in Fig. 4. As seen in the figure, the fatigue crack initiated from the casting defect located near the surface. As is the same with the case of material A, the casting defect near the surface with the size of approximately 1000 μm was the fatigue crack initiation site in the other two materials.

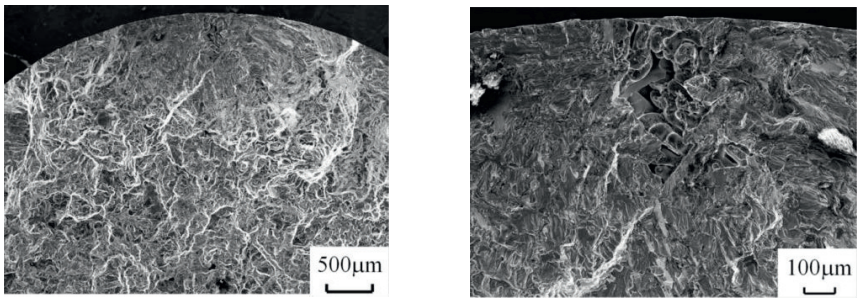

(a) low magnification (b) high magnification.

Fig.4 SEM micrographs showing crack initiation site of material A (σ_a=160MPa, N_f=5.4×10^4).

3.4. Distribution of casting defect size

The casting defect sizes were observed on several cross sections and the maximum defect size, √area, was estimated based on the extreme value statistics method proposed by Murakami (Murakami et al., 1989). As shown in

Fig.2, in material A and C, relatively large defects were observed separately far from each other. On the other hand, in material B, multiple small defects which existed very close to each other were observed frequently. When the distance between the neighboring defects is small, they should be equivalent to one combined large defect according to the size estimation method proposed by Murakami. When √area of the combined large defect was calculated using the criterion of defects combination proposed by Murakami, the √area of the material A, B and C were calculated as 1068, 1728 and 1153 μm, respectively.

3.5 Prediction of fatigue limit

Ueno et al. modified Murakami's equations and proposed the following equations to predict the fatigue limit, σ_w, for aluminum alloy:

$$\sigma_w = \frac{1.43(75+HV)}{(\sqrt{\text{area}})^{1/6}} \quad \text{where} \quad \sqrt{\text{area}} < 1400\ \mu\text{m} \tag{1}$$

$$\sigma_w = \frac{1.43(450+HV)}{(\sqrt{\text{area}})^{1/3}} \quad \text{where} \quad \sqrt{\text{area}} > 1400\ \mu\text{m} \tag{2}$$

where *HV* is the Vickers hardness and √area is the maximum defect size estimated by extreme value statistics. The fatigue limit of each material was predicted by the above equation using the hardness and maximum defect size shown in the section 3.1 and 3.4, respectively. Consequently, the predicted fatigue limits of material A, B and C were 85, 66 and 73 MPa, respectively.

4. Discussion

Experimental and predicted results of fatigue limit are summarized in Table 3. The predicted fatigue limit of material C based on Murakami's criterion of defects combination (see section 3.4), 73 MPa, is close to the experimental value, 75 MPa. On the other hand, in material B, the predicted fatigue limit, 66 MPa, is much lower than the experimental value, 80 MPa. In material B, it is considered that the maximum size of casting defect might have been over estimated using Murakami's criterion of defects combination. As mentioned previously, multiple defects which existed close to each other were observed frequently in material B. The multiple defects are regarded as one large defect when the distance is close to each other since they coalesce and become one large defect in the early stage of fatigue process. Fig.5 shows the schematic illustration of the method of defects combination. Applying the criterion of defects combination, the small defects are grouped into two defects, defect I and II. When the defects I and II are near enough to satisfy the criterion, they could be combined. By Murakami's criterion, the distance between defects I and II is smaller than √area of defects I or II, thus defects I and II are combined to defect III indicated by the dotted envelope in Fig.5 and defect III is regarded as one defect. Consequently, the maximum defect size was estimated as 1728 μm in material B as shown in the section 3.4. Here we propose another criterion. When the distance between defect *a* in the envelope I and defect *b* in the envelope II is larger than √area of defect *a* or *b*, the envelopes I and II are not combined and they are regarded to be independent defects. The extreme value statistics using this criterion is shown in Fig.6. In material B, √area of the maximum defect is estimated 1178 μm. Using this value, the predicted fatigue limit is calculated 79 MPa, which is close to the experimental value. √area of material A and C estimated using this method were calculated 1053 and 1153 μm, respectively, which are nearly the same or slightly smaller than that estimated using Murakami's criterion. This is because neighboring defects which existed close to each other were few in the materials A and C. The predicted fatigue limits of material A by the both criteria were excessively higher than the experimental value and it is an unconservative evaluation. Material A was sampled from the place which is far from the pouring gates where the cooling rate is the highest, but the place is near the cold shut where molten flow coalesces. It is considered that the low fatigue limit of material A is due to the cold shut. Further investigation is required to clarify the specific factors at the cold shuts.

5. Conclusion

The rotating bending fatigue tests of cast aluminum alloy A356 were conducted using the specimens sampled at different locations of a large scale component. The modified size estimation criterion for multiple defects gave better prediction of fatigue limit than the conventional criterion. The experimental fatigue limit in the materials near the cold shut was lower than the prediction.

Table 3 Experimental and predicted results of fatigue limit.

Material	Experimental			Fatigue life prediction using Ueno's equations			
				based on √area estimation by Murakami's criterion		based on √area estimation by this study's criterion	
	HV	DAS (μm)	σ_w (MPa)	√area (μm)	σ_w (MPa)	√area (μm)	σ_w (MPa)
A	116	57	65	1068	85	1053	86
B	108	84	80	1728	66	1312	79
C	90	96	75	1153	73	1153	73

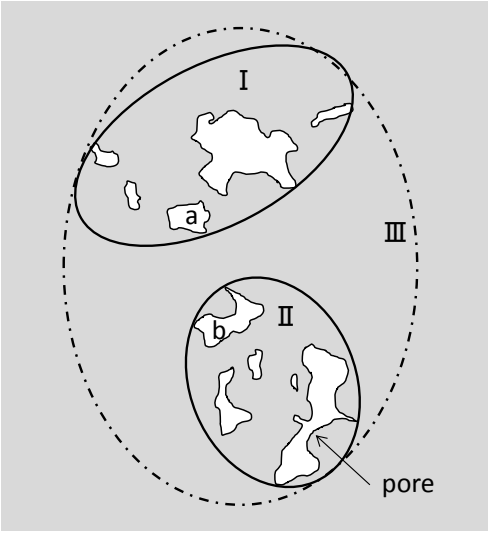

Fig.5 Schematic illustration of defects combination.

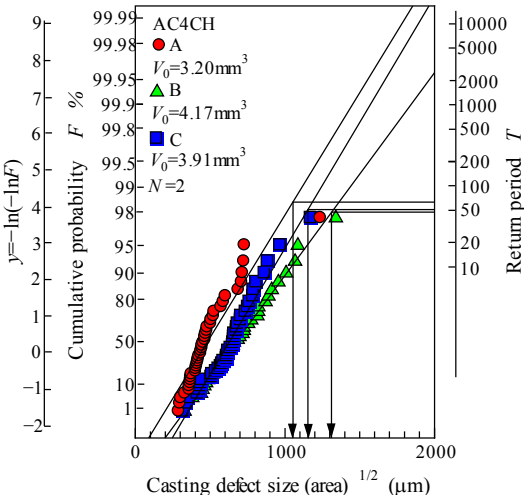

Fig.6 Extreme value distribution of casting defect size.

References

Murakami, Y., Kodama, S., Konuma, S., 1989. Quantitative Evaluation of Effects of Non-Metallic Inclusions on Fatigue Strength of High Strength Steels. I: Basic Fatigue Mechanism and Evaluation of Correlation between the Fatigue Fracture Stress and the Size and Location of Non-Metallic Inclusions, International Journal of Fatigue 11, 291-298.

Murakami, Y., Usuki, H., 1989. Quantitative Evaluation of Effects of Non-Metallic Inclusions on Fatigue Strength of High Strength Steels. II: Fatigue Limit Evaluation Based on Statistics for Extreme Values of Inclusion Size, International Journal of Fatigue 11, 299-307.

Ueno, A., Nishida, M., Miyakawa, S., Yamada, K., Kikuchi, S., 2012. Fatigue Limit Estimation of Aluminum Die-Casting Alloy by Means of √area Method, Proceedings of The 31st Symposium on Fatigue (in Japanese), 159-163.